Pharm Res (2012) 29:397–410
DOI 10.1007/s11095-011-0563-x

RESEARCH PAPER

Behavior of Monoclonal Antibodies: Relation Between the Second Virial Coefficient (B_2) at Low Concentrations and Aggregation Propensity and Viscosity at High Concentrations

Shuntaro Saito • Jun Hasegawa • Naoki Kobayashi • Naoyuki Kishi • Susumu Uchiyama • Kiichi Fukui

Received: 21 March 2011 / Accepted: 3 August 2011 / Published online: 19 August 2011

ABSTRACT

Purpose To investigate relationship between second virial coefficient B_2 and viscosity and aggregation propensity of highly concentrated monoclonal antibody (MAbs) solutions.

Methods Intermolecular interactions of 3 MAbs solutions with varying pH were characterized according to B_2 estimated by analytical ultracentrifugation sedimentation equilibrium with initial loading concentrations <10 mg/mL. Viscosity measurements and stability assessments of MAb solutions at concentrations higher than 100 mg/mL were conducted.

Results B_2 of all MAb solutions depended on solution pH and have qualitative correlation with viscosity and aggregation propensity. The more negative the B_2 values, the more viscous the solution, acquiring increased propensity to aggregate. Solutions with B_2 values of $\sim 2 \times 10^{-5}$ mL·mol/g^2 acquire similar viscosity and aggregation propensity regardless of amino acid sequences; for solutions with negative B_2 values, viscosity and aggregation propensity differed depending on sequences. Results suggest attractive intermolecular interactions represented by negative B_2 values are influenced by surface properties of individual MAbs.

Conclusions B_2 can be used, within certain limitations, as an effective indicator of viscosity and aggregation propensity of highly concentrated MAb solutions.

KEY WORDS aggregation · analytical ultracentrifugation sedimentation equilibrium · monoclonal antibody · second virial coefficient · viscosity

INTRODUCTION

Several different therapeutic antibodies have recently entered the market, and many more are currently in clinical trials for the treatment of diseases such as cancer, infectious diseases, allergies, autoimmune diseases, cardiovascular diseases, and inflammation (1). Antibody treatment generally involves administration of high doses of antibodies. Therefore, intravenous (IV) administration is often the first choice for an administration route. IV administration, however, requires a significant amount of time, and sufficient care needs to be provided by skilled healthcare professionals. Therefore, patients must receive treatments at clinics specializing in antibody treatment. More convenient administration routes such as subcutaneous (SC) and intramuscular (IM) routes are favorable because they would reduce the burden on patients, and for both routes, the maximum injection volume should be below approximately 1.5 mL per dose. However, for achieving a therapeutic effect, an antibody solution with a concentration as high as 100 mg/mL needs to be administered in a single injection.

Development of high-concentration antibody solutions is challenging because unfavorable phenomena such as

Electronic Supplementary Material The online version of this article (doi:10.1007/s11095-011-0563-x) contains supplementary material, which is available to authorized users.

S. Saito · J. Hasegawa · N. Kobayashi · N. Kishi
Analytical & Quality Evaluation Research Laboratories
Daiichi Sankyo Co., Ltd.
1-16-13, Kitakasai
Edogawa-ku, Tokyo 134-8630, Japan

S. Saito · S. Uchiyama · K. Fukui (✉)
Department of Biotechnology, Graduate School of Engineering
Osaka University
2-1 Yamadaoka
Suita, Osaka 565-0871, Japan
e-mail: kfukui@bio.eng.osaka-u.ac.jp

increased viscosity and aggregation are frequently induced by increases in the concentration of antibody solutions (2,3). These properties introduce challenges in effective manufacture, formulation development, analytical characterization, and administration of therapeutic antibodies. Although direct measurements of the viscosity and aggregation propensity using high-concentration solutions provide useful information, the preparation of such solutions remains challenging, even on a small scale. In addition, it is technically difficult to measure the very weak intermolecular interactions ($K_d \sim$ mM) that become dominant at concentrations above 100 mg/mL (4,5). Furthermore, even in cases where successful measurements have been made, interpretation of the data is extremely difficult since no concrete theory regarding this has yet been established. For example, the contribution of the repulsive interactions due to the excluded volume effects becomes more significant (6,7), and the shorter interactive intermolecular distances changes the short-range intermolecular interactions as the concentration increases. This causes the intermolecular interaction profile to become more complicated (8,9). In practice, an analytical technique for estimating potential issues involved in developing high-concentration antibody solutions is strongly required.

Reversible self-association of antibodies is thought to induce high viscosity (5,10,11) and aggregation at high concentrations (12–14). The mechanism of self-association at the molecular level is complicated. Different types of intermolecular forces are involved in reversible intermolecular interactions, such as electrostatic interactions, van der Waals forces, and hydrophobic interactions (15). Environmental factors such as pH, ionic strength, and additives can alter the intermolecular interaction profile drastically (14,16–18). In our recent study, we reported that ionic strength has a significant effect on the reversible self-association of an antibody, leading to liquid-liquid phase separation and an increase in viscosity at low ionic conditions (19). These studies indicate that the selected formulation is critical for reducing viscosity (5,20). As for the relationship between self-association and aggregation, Wu *et al.* reported that hydrophobic patches on the surface of monoclonal antibody (MAb) molecules cause low solubility and induce aggregation due to self-association (21). Primary and higher-order structures of MAbs are also important factors, and different types of self-association have been reported such as Fab–Fab and Fc–Fc interactions (22). Kanai *et al.* reported that self-association between Fab fragments is responsible for high viscosity at high concentrations where electrostatic interactions are a major driving force for self-association (11). However, this is not always true for all MAbs. The types and strength of interactions are highly dependent on the amino acid sequence of the MAbs.

Several approaches have been used to evaluate the intermolecular interactions (10,13,15,23). The second virial coefficient (B_2) is a parameter that represents the degree of intermolecular interactions in dilute solutions. This parameter can thus be used as an indicator of intermolecular interaction. It is generally understood that a positive B_2 value implies the presence of repulsive intermolecular interactions, while a negative B_2 value indicates the presence of attractive intermolecular interactions (24,25). B_2 values of MAbs solutions have been estimated using static light scattering (SLS) (26–28) and self-interaction chromatography (SIC) (29,30). The interaction parameter (k_d), which relates to B_2, can be derived from dynamic light scattering (DLS) (12,28). Instead of making direct measurements, such as quantifying the extent of aggregation and viscosity, the use of an indicator for intermolecular interactions that can be estimated with a small amount of sample has been proposed in order to make predictions of solution behavior at high concentrations of MAbs. SIC provides a means for measuring B_2 values under different solution conditions by an automated HPLC technique. There is a concern, however, that B_2 values determined from SIC do not correspond to the interaction of proteins in solution because SIC measures the interaction of molecules in solution with molecules immobilized on the column matrix. In addition, degradation and conformational changes in MAbs that occur during the preparation of columns and nonspecific interactions of MAbs with the column matrix are also of concern.

Analytical ultracentrifugation sedimentation equilibrium (AUC-SE) is a conventional technique for determination of the apparent molecular weight ($M_{W,app}$). This method is applicable to samples over a wide range of concentrations and of various solvent compositions (4,5). AUC-SE evaluates the equilibrium concentration gradient in the cell being centrifuged, and typically a 3-fold or higher concentration region relative to the initial loaded concentration can be generated near the bottom of the cell at sedimentation equilibrium.

In this study, we first carried out AUC-SE of three MAbs at nine different concentrations for the establishment of a concentration range suitable for the estimation of B_2. Then, B_2 was determined in solutions of varying pH for three different MAbs. We also measured the viscosity and aggregation propensity of MAb solutions at high concentrations. All MAbs showed a marked B_2 trend as a function of pH, and this is in good qualitative agreement with both the viscosity and the aggregation propensity. Our present study demonstrates that B_2 values derived from AUC-SE using antibody solutions below 10 mg/mL as the initial loading concentration can be a reliable qualitative indicator of MAb behaviors at high concentrations.

MATERIALS AND METHODS

Materials

The humanized monoclonal antibody A (IgG_1 subclass, MAb-A), B (IgG_1 subclass, MAb-B), and C (IgG_1 subclass, MAb-C) were produced and highly purified at Daiichi Sankyo Co., Ltd., Tokyo, Japan. All MAbs are humanized IgG_1 but recognize different antigens. The theoretical isoelectric points (pI) of MAb-A, MAb-B, and MAb-C are 6.7, 8.9, and 8.8, respectively. The molecular weights (M_W) of MAb-A, MAb-B, and MAb-C calculated from amino acid sequences with 2 oligosaccharide chains ($M_{W,cal}$) are 150, 147, and 148 kDa, respectively. All MAbs were stocked at –80°C in 10 mM sodium citrate buffer and 140 mM sodium chloride (pH 6). MAbs were dialyzed against the desired buffers (pH 5, 6, 7, and 8) before use, and the concentrations were determined based on the absorbance at 280 nm. MAbs were diluted to adjust the desired concentration prior to each experiment. Sodium chloride was purchased from Wako Pure Chemical Industries, Ltd. (Osaka, Japan), and sodium phosphate and sodium acetate were purchased from Kanto Chemical Co. (Tokyo, Japan). Four buffers of different pH were prepared. The composition at pH 5 was 10 mM sodium acetate buffer containing 140 mM NaCl, and that at pH 6, 7, and 8 was 10 mM sodium phosphate buffer containing 140 mM NaCl.

Sedimentation Equilibrium Studies

Sedimentation equilibrium was carried out using XL-I (Beckman Coulter, Inc., Brea, CA). A volume of 100 μL of each solution was applied into the sample sectors of six holes, charcoal-filled epon centerpiece (1.2 cm) with sapphire windows, and 100 μL of reference solutions were applied into the reference sectors. The runs were carried out at 11,000 rpm at 20°C by using the An-60Ti rotor. The concentration gradient was acquired by Rayleigh interference (IF) optics. The concentration gradients were acquired at two-hour intervals and were judged to be at equilibrium when the three successive gradients were completely superimposed. $M_{W,app}$ was estimated by nonlinear least-squares fitting of data according to Eq. 1 using the program Microcal Origin, ver 4.1:

$$c(r) = c_0 \exp\left[\frac{M_{W,app}(1-\nu\rho)\omega^2}{2RT}\left(r^2 - r_o^2\right)\right] + \text{Baseline} \quad (1)$$

where, $c(r)$ (mg/mL) is the protein concentration at the radial position r (cm), c_0 is the protein concentration at the reference radial position r_0, v (cm^3/g) is the partial specific volume of solute, ρ (g/cm^3) is the solvent density, ω (rad/s) is the angular velocity, T (K) is the absolute temperature, and R is the gas constant. Partial specific volume and solvent density were calculated using the software Sednterp (31). Partial specific volumes of MAb-A, MAb-B, and MAb-C according to the amino acid compositions were 0.7261, 0.7272, and 0.7275 cm^3/g, respectively. Buffer densities were 1.00521 g/cm^3 for 10 mM sodium acetate buffer containing 140 mM NaCl, and 1.00461 g/cm^3 for 10 mM sodium phosphate buffer containing 140 mM NaCl.

B_2 was obtained from the slope when the inverse of $M_{W,app}$ was plotted against the concentration according to Eq. 2, where M_W is the weight average molecular weight at infinite dilution and c is the initial loading concentration.

$$\frac{1}{M_{W,app}} = \frac{1}{M_W} + 2B_2c \quad (2)$$

Estimation of Concentration Dependence of Diffusion Coefficient by DLS

A 20 μL volume of 1.0, 2.0, 4.0, 6.0, 8.0, and 10 mg/mL sample solutions (after filtration with a 0.22-μm filter) was applied to 384-well optical clear-bottom microtiter plates. Following centrifugation at 50g for 3 min to remove bubbles, the diffusion coefficient was measured using a DynaPro Plate Reader (Wyatt Technology Corp., Santa Barbara, CA) at 20°C. The interaction parameter (k_d) was calculated using Eq. 3, where D_m is the measured diffusion coefficient, D_s is the diffusion coefficient at infinite dilution, and c is the concentration of MAb (mg/mL) (12,28).

$$D_m = D_s(1 + k_d c) \quad (3)$$

where k_d represents the thermodynamic term of B_2 and the hydrodynamic term of (ξ_1+v) as shown in the following equation:

$$k_d = 2B_2M_W - (\xi_1 + \nu) \quad (4)$$

where, ξ_1 is obtained from the virial expansion of the concentration-dependent frictional coefficient.

Viscosity Measurement

Samples were concentrated and buffer exchanged using a Vivapore-2 concentrator device (Sartorius AG, Goettingen, Germany). Following centrifugal filtration (filter size: 0.45 μm), samples were adjusted to a concentration of 150 mg/mL. The concentrations of the sample were determined by size exclusion chromatography (SEC) using reference solutions for the respective MAbs; the concentrations of these solutions were calculated based on the absorbance at 280 nm. SEC analysis was conducted with a TSK gel $G3000SW_{XL}$ (TOSOH Co., Tokyo, Japan)

column using the mobile phase of 30 mM sodium phosphate buffer and 300 mM NaCl (pH 6.7) at a flow rate of 1.0 mL/min and a column temperature of 20°C. The sample solution was diluted to approximately 1.0 mg/mL, and 50 μL of each solution was injected for analysis. The peak area was monitored at 280 nm using a UV detector. Viscosity was measured by VROC (RheoSense, Inc., San Ramon, CA) at the controlled temperature of 20°C (19).

Stability Study

Volumes of 100 μL of 100 mg/mL antibody solutions were applied in triplicate to a 96-well polypropylene polymerase chain reaction (PCR) plate with cap. Plates were stored at 40°C for 2 or 4 weeks. Each sample was diluted to 1.0 mg/mL, and their aggregation profiles were analyzed by SEC, DLS, and turbidity analysis. It was confirmed that there was no change in concentration during storage.

SEC

Diluted samples of 1.0 mg/mL were filtered using 96-well filtration plates (0.45 μm). The SEC analysis was carried out with a TSK gel G3000SW$_{XL}$ (TOSOH Co.) column, using 30 mM phosphate buffer and 300 mM NaCl (pH 6.7) as the mobile phase at a flow rate of 1.0 mL/min and a column temperature of 25°C. A 50 μL volume of each solution was injected in the column. The peak area was monitored at 280 nm by a UV detector. The percentage of aggregates, determined from the sum of peaks eluted in front of the monomer peak, was estimated by dividing the aggregate peak area by the total peak area. The rate of increase in the aggregates, the aggregation rate (% per week), was estimated from least-squares fitting of the time dependence of the percentage of aggregates.

DLS

Volumes of 20 μL of samples were applied to 384-well optical clear-bottom microtiter plates. Following centrifugation at 50*g* for 3 min to remove the large particulates and bubbles, the average hydrodynamic diameter was measured at 20°C using a DynaPro Plate Reader.

Turbidity Measurement

Volumes of 200 μL of samples were applied to 96-well optical clear-bottom microtiter plates. The turbidity was monitored at 350 nm by a SpectraMax M2 plate reader (Molecular Devices, Sunnyvale, CA). The optical path length d was determined experimentally based on the published method (32). The turbidity of the solution was calculated according to the following equation:

$$\text{Turbidity (AU/cm)} = \frac{A_{350}}{d} \tag{5}$$

where A_{350} is the absorbance at 350 nm.

Thermal Stability Assessment by DLS

Samples were diluted with buffers to a concentration of 1.0 mg/mL. Volumes of 20 μL of sample solutions after filtration (0.22 μm) were applied to 384-well optical clear-bottom microtiter plates. Following centrifugation at 50*g* for 3 min to remove bubbles, samples were covered with 10 μL of mineral oil to prevent evaporation. Thermal stability assessments were performed using a DynaPro Plate Reader. The average hydrodynamic diameter (d_H) was acquired by DYNAMICS Ver. 7.0.2 (Wyatt Technology Corp.) The plate temperature was increased from 50°C to 75°C at temperature increment of 1°C. The plate temperature was monitored during the assay. The d_H at each temperature was measured after the plate temperature became stable at the set temperatures. Consequently, the average heating rate was approximately 0.032°C/min ± 0.005°C/min. T_m^* was defined as the temperature where the average d_H drastically jumps from the value of the MAb monomer (approximately 10 nm) to that over 200 nm, which corresponds to a large aggregate.

RESULTS

B_2 Measurement by AUC-SE

Figure 1 shows the concentration dependence of $1/M_{W,app}$, from which B_2 could be estimated for all MAbs. It is generally understood that a positive B_2 value, from Eq. 2, is obtained from an increase in $1/M_{W,app}$ with an increase in concentration. This indicates the presence of repulsive intermolecular interactions. Negative B_2 values obtained from a decrease in $1/M_{W,app}$ and an increase in concentration indicate the presence of attractive intermolecular interactions. Three MAbs showed significant differences in the concentration dependences of $1/M_{W,app}$. The $1/M_{W,app}$ of MAb-A decreased as the concentration increased, indicating the presence of attractive intermolecular interactions. On the other hand, $1/M_{W,app}$ of MAb-C increased as the concentration increased, indicating the presence of repulsive intermolecular interactions. The concentration dependences of $1/M_{W,app}$ were successfully fitted using a linear model for MAb-A and MAb-C with the correlation coefficients (R) of $R>0.95$ in the tested concentration range from 1 to 12 mg/mL (see Supplementary Material for the

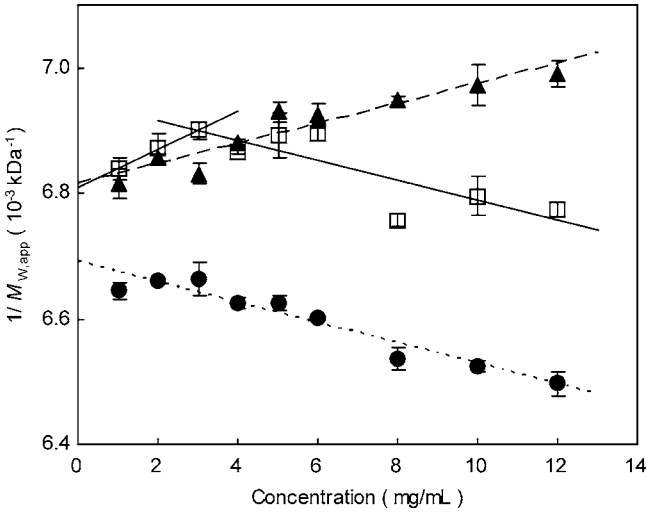

Fig. 1 Concentration dependence of $1/M_{W,app}$ obtained from AUC-SE. The results of MAb-A (●), MAb-B(□), and MAb-C (▲) in 10 mM citrate buffer containing 140 mM NaCl (pH6) are shown. Regression lines are generated from the least-squares fitting of the concentration dependence of $1/M_{W,app}$. The data obtained over the entire concentration range 1 to 12 mg/mL are used for MAb-A and MAb-C. Those with lower concentrations 1 to 3 mg/mL or higher concentrations 4 to 12 mg/mL are used for MAb-B. The error bar was estimated from 3 independent experiments under the same conditions. The intercepts of the regression line is $1/M_W$ according to Eq. 2, and the values of MAb-A, MAb-B, and MAb-C were 6.69, 6.81, and 6.81×10^{-6} kDa^{-1}, respectively, corresponding to M_W values of 150, 147, and 147 kDa, respectively.

residual plots). The concentration dependence of $1/M_{W,app}$ of MAb-B was different from that of MAb-A and MAb-C; $1/M_{W,app}$ of MAb-B was observed to increase in the concentration range of 1 to 3 mg/mL and decrease in the higher concentration range of 4 to 12 mg/mL. Obviously, a linear model could not be applied to MAb-B over the entire concentration range examined. Then, the concentration range was divided into two ranges, and linear regressions were calculated for each concentration range. The lower range was defined as 0 to 3 mg/mL, at which the fitting was successful as confirmed by $R=1.00$. The higher range was defined as 4 to 12 mg/mL. The linear fitting using the data at higher concentration range provided a slope that is clearly different from the slope obtained for the lower range. Thus, two B_2 values were obtained from the different concentration ranges. The M_W values of MAb-A, MAb-B, and MAb-C at infinite dilution obtained by AUC-SE according to Eq. 2 were 150, 147, and 147 kDa, respectively. As for MAb-B, the B_2 value obtained for the lower concentration range was employed. All M_W values were in good accordance with $M_{W,cal}$ values (150, 147, and 148 kDa). These results indicate that concentration dependences of $1/M_{W,app}$ for all MAbs are represented as linear models and that reliable B_2 values can be obtained for the concentrations examined.

Thus, in the present study, subsequent AUC-SE measurements of MAb-A and MAb-C were carried out at 1, 5, and 10 mg/mL, from which $1/M_{W,app}$ values for B_2 were estimated. AUC-SE measurements of MAb-B were performed at 1, 2, 3, 5, 7.5, and 10 mg/mL. B_2 values of MAb-B were estimated from the concentration dependence of $1/M_{W,app}$ values at 1, 2, and 3 mg/mL, or the concentration dependence of $1/M_{W,app}$ values at 5, 7.5, and 10 mg/mL.

pH Dependence of B_2

B_2 and k_d have been investigated as a function of solution pH because pH is recognized as an important parameter influencing intermolecular interactions by changing the electrostatic environment of proteins. In fact, B_2 and k_d are known to vary according to pH (10,13,33). In the present study, we also investigated the effect of pH on the intermolecular interactions of MAbs. B_2 determined by AUC-SE at different pH values is shown in Fig. 2. All three

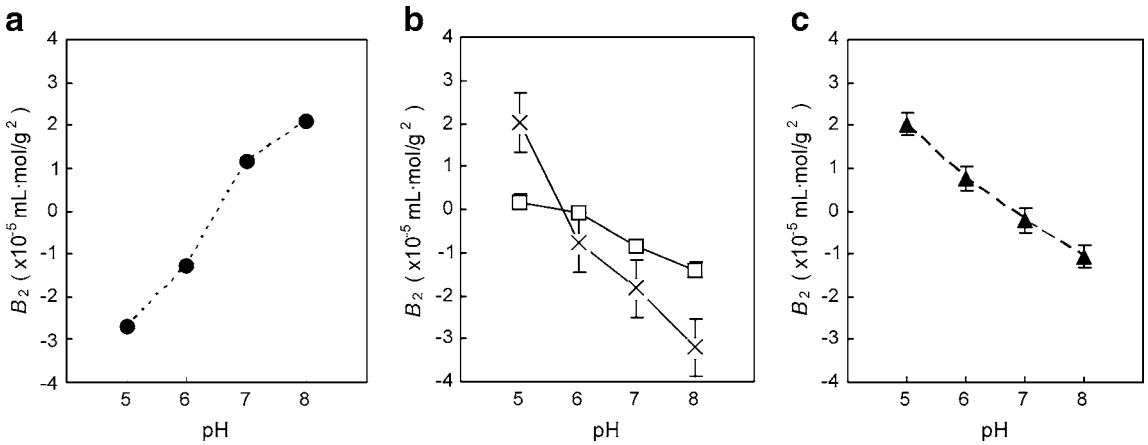

Fig. 2 pH dependence of second virial coefficient (B_2) for MAb-A (**a**), MAb-B (**b**), and MAb-C (**c**). B_2 was obtained from the concentration dependence of $M_{W,app}$ at 3 different concentrations in 10 mM sodium acetate buffer containing 140 mM NaCl (pH 5) or 10 mM phosphate buffer containing 140 mM NaCl (pH 6, 7, and 8). B_2 of MAb-A and MAb-C were obtained from concentrations 1, 5, and 10 mg/mL. B_2 of MAb-B was obtained from the 2 concentration ranges at 1, 2, and 3 mg/mL (×) and 5, 7.5, and 10 mg/mL (□).

MAbs clearly show remarkable pH dependence of B_2 with only small standard deviations estimated from three repeated experiments. B_2 values of MAb-A increased with an increase in pH; they were negative at pH 5 and 6 and positive at pH 7 and 8. These results indicate that attractive intermolecular interactions dominate at pH 5 and 6, while repulsive intermolecular interactions dominate at pH 7 and 8. In contrast, B_2 values of MAb-C decreased as the pH increased. As for MAb-B, the B_2 values were estimated from two concentration ranges. Obviously, the pH dependences of both B_2 values were qualitatively comparable: both B_2 values were observed to decrease with an increase in pH. On the other hand, the absolute magnitudes of B_2 values from the two different concentration ranges were different from each other at all pH values examined. This indicates that the magnitude of the intermolecular interactions depends upon the concentration. These results indicate that attractive intermolecular interactions of MAb-B and MAb-C become dominant at high pH.

k_d Measurement by DLS

DLS is widely used for estimating intermolecular interactions. It has the advantages of high throughput and operability and requires small samples. DLS has been employed to investigate k_d based on the concentration dependence of the diffusion constant using Eq. 3. k_d is regarded as the factor that reflects the extent of intermolecular interactions (12,28).

The results indicate that all MAbs show decreases in D_m with increased concentration under all pH conditions, resulting in negative k_d values. As shown in Fig. 3, MAb-A has a more negative k_d value as the pH decreases. In contrast, k_d of MAb-B and MAb-C becomes gradually less negative as the pH decreases, except for the k_d of MAb-C at pH 8. Consequently, the k_d value of MAb-C was minimal at pH 7.

Thermal Stability Assessment by DLS

Aggregation induced by thermal unfolding can be monitored by measuring the average d_H value with elevated temperatures. The diameter of a MAb monomer is approximately 10 nm, while above the T_m^*, the observed diameter is greater than several hundred nm, indicating the formation of large aggregates. Figure 4a–c illustrate the average d_H with elevated temperatures for three MAbs with different pH values. The T_m^* of MAb-A is clearly dependent on pH (Fig. 4d). The lowest thermal stability was confirmed at pH 5 and was found to be enhanced according to the following trend: pH 5<pH 6<pH 7=pH 8. Herein, MAb-A showed unique behavior at pH 7 and 8, where d_H was observed to first increase to approximately 100 nm with a subsequent jump to more than 200 nm at higher temperatures. The higher temperature was defined as T_m^* of MAb-A. No significant difference among T_m^* values was confirmed in both MAb-B and MAb-C for all pH values investigated.

Viscosity of MAb Solutions at High Concentration

The viscosities of the three MAbs at a concentration of 150 mg/mL were measured at different pH values. Figure 5 indicates that the viscosities of all MAb solutions are clearly dependent upon the pH of the solution. The viscosity of the MAb-A solution is higher at low pH (pH 5 and 6). In contrast, the pH dependencies of MAb-B and MAb-C are different from that of MAb-A, where viscosity is markedly increased at high pH. In all cases, the quantities of aggregates were unchanged when observed by SEC (data

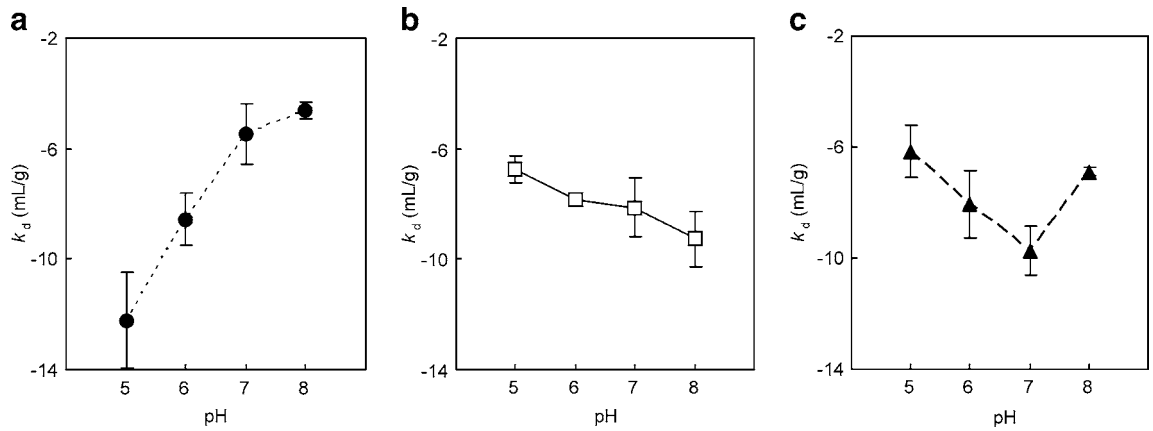

Fig. 3 pH dependence of k_d based on DLS. k_d was obtained from 6 different concentrations—1.0, 2.0, 4.0, 6.0, 8.0, and 10.0 mg/mL for 3 MAbs. MAb-A (**a**), MAb-B (**b**), and MAb-C (**c**) were formulated in 10 mM sodium acetate buffer containing 140 mM NaCl (pH 5) and 10 mM phosphate buffer containing 140 mM NaCl (pH 6, 7, and 8). The error bar was estimated from 3 independent experiments performed under the same conditions.

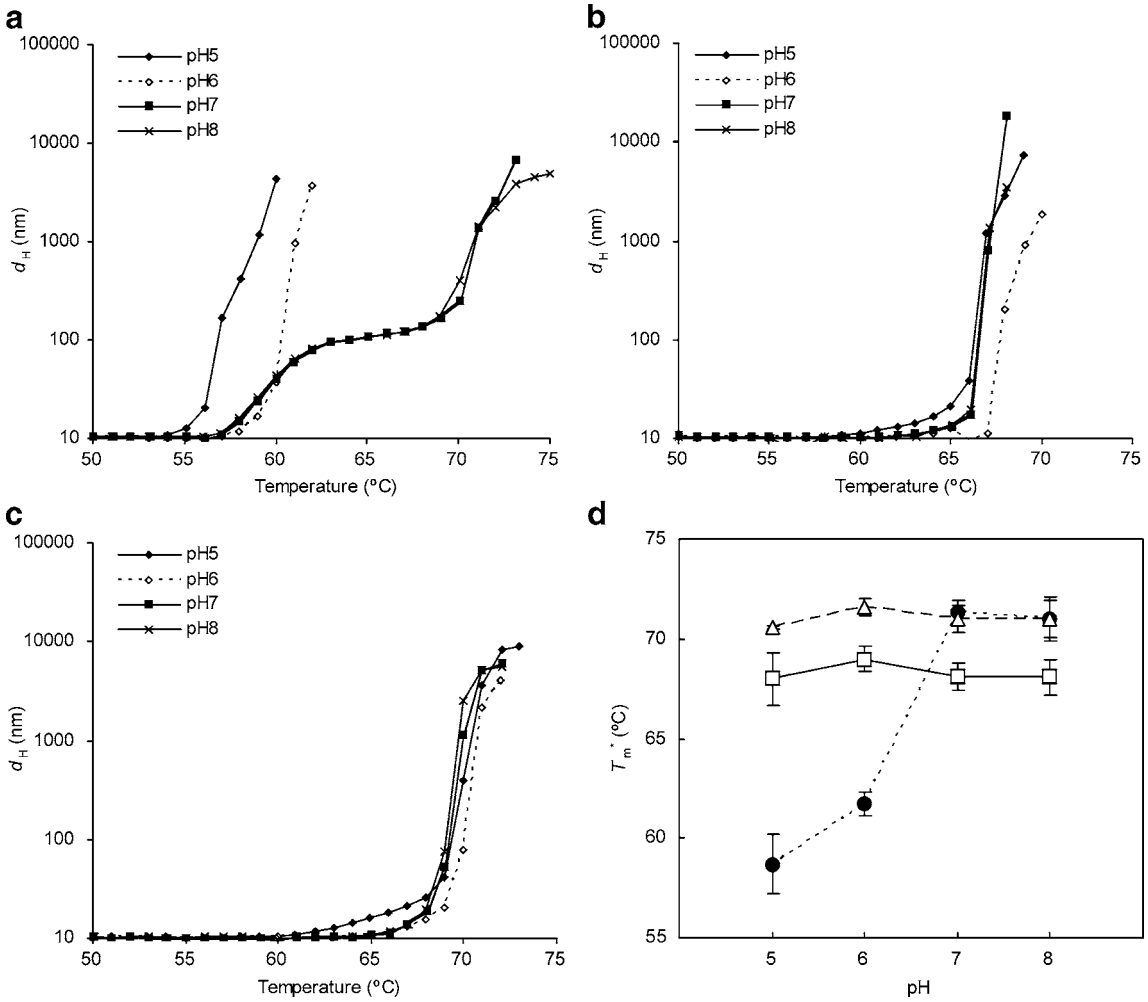

Fig. 4 pH dependence of thermal stability based on DLS. The hydrodynamic diameter d_H was obtained by elevating the temperature from 50°C to 75°C. MAb-A (**a**), MAb-B (**b**), and MAb-C (**c**) were formulated in 10 mM sodium acetate buffer containing 140 mM NaCl (pH 5) and 10 mM phosphate buffer of 140 mM NaCl (pH 6, 7, and 8). T_m^* values are plotted as a function of pH for MAb-A (●), MAb-B(□), and MAb-C (Δ) (**d**). The error bar was estimated from 3 independent experiments performed under the same conditions.

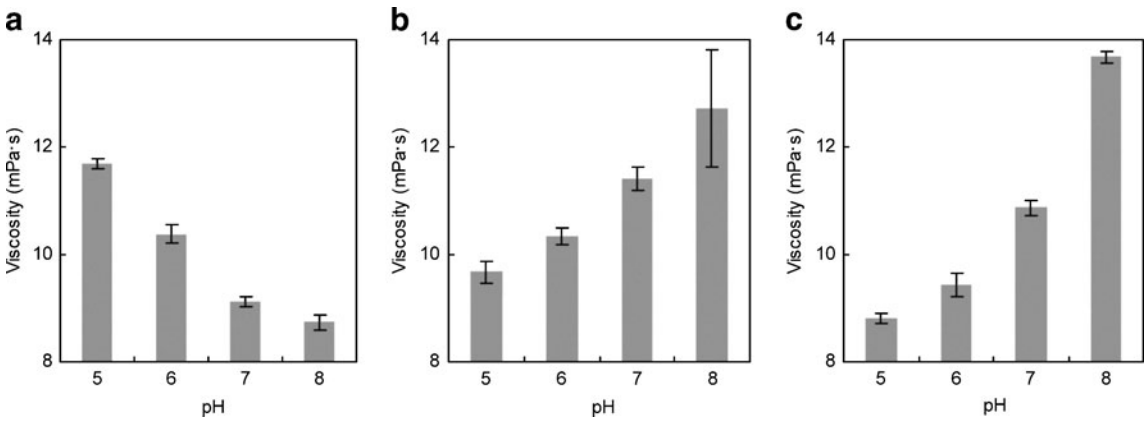

Fig. 5 pH dependence of viscosity. Viscosity was measured using MAb solutions with a concentration of 150 mg/mL. MAb-A (**a**), MAb-B (**b**), and MAb-C (**c**) were formulated in 10 mM sodium acetate buffer containing 140 mM NaCl (pH 5) and 10 mM phosphate buffer containing 140 mM NaCl (pH 6, 7, and 8). The error bar was estimated from 3 independent experiments performed under the same conditions.

not shown), indicating that the differences in viscosity cannot be attributed to differences in the aggregate content.

Aggregation Propensities of Highly Concentrated MAbs During Storage

Stability assessment under accelerated conditions (40°C) was carried out for highly concentrated solutions (100 mg/mL) of all three MAbs. In this study, changes in the aggregate profile during storage were evaluated by SEC, DLS, and turbidity in order to monitor the wide ranges of aggregates in terms of size (34). SEC is widely used for the evaluation of small soluble aggregates (invisible aggregates of sizes less than 0.1 μm) that pass through the SEC column. DLS is suitable for the detection of sub-micron particles (subvisible aggregates of sizes between 0.1 to 1 μm: subvisible). Turbidity measurements are capable of detecting insoluble aggregates (visible aggregates of sizes greater than 1 μm).

Figure 6 illustrates the amount of soluble aggregates obtained and the rate of aggregation increase per week as estimated from SEC measurements. The amount of small soluble aggregates was observed to increase for all MAbs at 40°C. MAb-A clearly shows pH dependence where the aggregation rate accelerates as the pH decreases. In contrast, the pH dependencies of the aggregation rates for MAb-B and MAb-C accelerate as the pH increases.

The results of turbidity measurements are summarized in Table I. The absorbance increase due to particulate formation was not observed for all MAbs. The formation of submicron-sized particles represented by d_H on DLS is also shown in Table I. No significant change in d_H was observed during storage. These results indicate that neither submicron particulates nor insoluble aggregates are formed under any pH conditions.

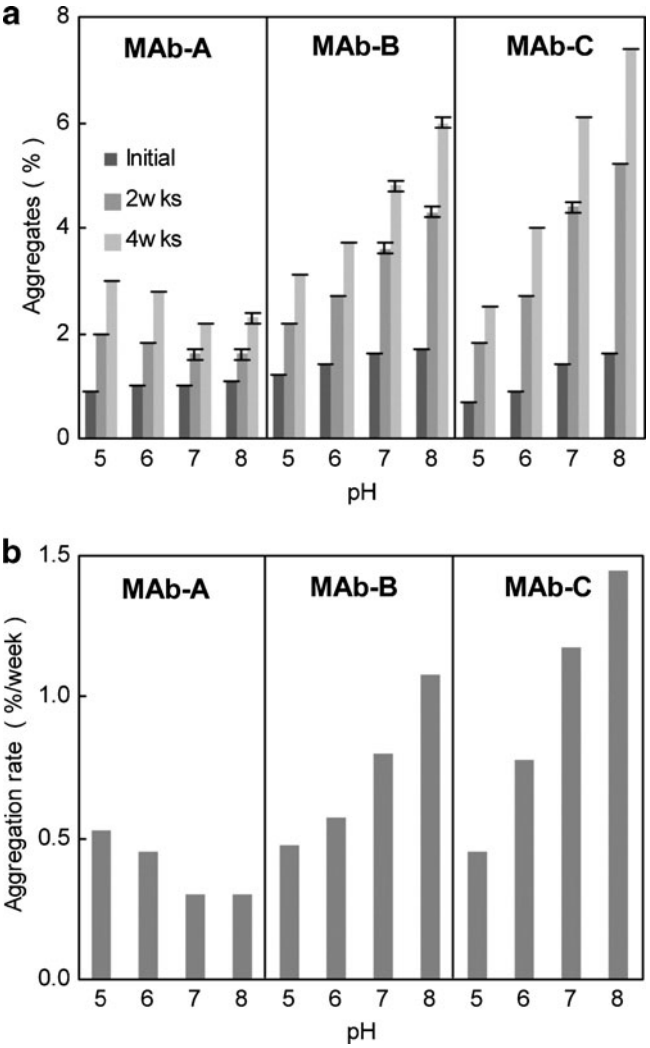

Fig. 6 Quantification of aggregates by SEC. MAbs were stored at 40°C at 4 different pHs. (**a**) Aggregates (%) were measured after 0, 2, and 4 weeks of storage. The error bar was estimated from 3 independent experiments performed under the same conditions. (**b**) The increase in the rate of aggregation was estimated from the increase in the population of aggregates (%) per week.

DISCUSSION

Correlation Between Intermolecular Interaction at Low Concentration and Physical Properties at High Concentration

The purpose of the present study was to investigate the relationship between B_2 and viscosity or aggregation propensity so that one can select MAbs with superior physical properties such as low viscosity and low aggregation propensity. This will enable us to optimize formulations at the high concentrations required for alternative routes of administration. Direct measurements of viscosity and aggregation propensity using highly concentrated solutions are desirable. However, it is difficult to prepare highly concentrated solutions, and large amounts of samples are required for the measurements. These drawbacks reduce the numbers of candidate MAbs and formulation parameters for comprehensive characterization and cause MAbs to be selected in the context of specific formulations for further development without sufficient data on the physical properties of the MAbs. Instead of direct measurements, estimations of viscosity and aggregation at high concentrations have been performed from the solution properties of diluted solutions.

There are two approaches for characterizing the intermolecular interactions of MAbs. The first approach is to measure the effective intermolecular interactions under physiological conditions within a variety of realistic formulations for therapeutic MAbs. This approach is suitable for measuring the physical properties of proteins in the native state under isotonic solution conditions at ambient

Table I Stability Assessments Based on Turbidity and the Hydrodynamic Diameter

		Turbidity (AU/cm)		d_H (nm)	
		Initial	40°C	Initial	40°C
MAb-A	pH5	0.14 ± 0.01	0.12 ± 0.00	10.6 ± 0.1	10.9 ± 0.1
	pH6	0.14 ± 0.00	0.13 ± 0.00	10.6 ± 0.1	10.7 ± 0.0
	pH7	0.14 ± 0.00	0.12 ± 0.00	10.7 ± 0.2	11.0 ± 0.0
	pH8	0.14 ± 0.01	0.13 ± 0.00	10.5 ± 0.1	11.6 ± 0.4
MAb-B	pH5	0.14 ± 0.01	0.13 ± 0.00	10.4 ± 0.0	10.5 ± 0.1
	pH6	0.13 ± 0.01	0.13 ± 0.00	10.4 ± 0.1	10.5 ± 0.0
	pH7	0.13 ± 0.00	0.13 ± 0.00	10.5 ± 0.1	10.7 ± 0.1
	pH8	0.13 ± 0.00	0.13 ± 0.00	10.5 ± 0.1	11.1 ± 0.1
MAb-C	pH5	0.14 ± 0.01	0.13 ± 0.00	10.4 ± 0.0	10.8 ± 0.2
	pH6	0.13 ± 0.00	0.13 ± 0.00	10.4 ± 0.1	10.8 ± 0.5
	pH7	0.13 ± 0.00	0.13 ± 0.00	10.6 ± 0.1	10.6 ± 0.2
	pH8	0.13 ± 0.01	0.13 ± 0.00	10.5 ± 0.0	11.3 ± 0.5

MAbs were stored at 40°C for 4 weeks at 4 different pH values. The hydrodynamic diameter d_H was obtained from DLS. The error value was estimated from 3 independent experiments performed under the same conditions

temperature. Therefore, this approach is applicable for the screening of specific parameters that are required for formulation development. The second approach is to explore the factors influencing the physical properties under non-physiological conditions that are not used in the formulation and/or during the storage of therapeutic MAbs, such as low ionic strength and high temperature. This approach is useful for elucidating the types and mechanisms of intermolecular interactions because the potential intermolecular interactions that are hardly detectable under physiological conditions are enhanced.

We primarily used the first approach with respect to development of MAb pharmaceuticals. The relationships between intermolecular interactions at low concentrations and (1) viscosity and (2) aggregation propensity at high concentrations were investigated under physiological conditions. B_2 values obtained by AUC-SE were investigated to assess the extent of intermolecular interactions occurring at low concentrations of MAbs. As a first step toward estimation of B_2 under different conditions, the concentration dependencies of $1/M_{W,app}$ were precisely observed at concentrations between 1 and 12 mg/mL. With regard to MAb-A and MAb-C, the $1/M_{W,app}$ values were observed to change linearly as the concentrations increased. This observation is supported by the fact that concentration dependences of $1/M_{W,app}$ in the whole concentration range could be fitted to a linear regression with high R values. In contrast, it was unexpectedly found that the concentration dependence of $1/M_{W,app}$ for MAb-B was required to be described by two linear regressions with different slopes and intercepts. Fitting of the values at concentrations ranging from 1 to 3 mg/mL and from 4 to 12 mg/mL to linear regressions successfully provided two different B_2 values as indicated by the residual plot (see Supplementary Material). In the case of MAb-B, attractive interactions that contribute to the association are negligible, and repulsive interactions are essential within the concentration range of 1 to 3 mg/mL. On the other hand, attractive interactions become gradually dominant above 4 mg/mL. This change in the type and/or sign of intermolecular interactions (as indicated by the B_2 values) with increasing concentration leads to the unique concentration dependence of $1/M_{W,app}$. Importantly, although the two B_2 values of MAb-B differ from each other under all pH conditions, they similarly vary as the solution pH changes (Fig. 2b). Hence, the relationship of B_2 with pH showed a similar pattern in the concentration ranges 1 to 3 mg/mL and 4 to 12 mg/mL (Fig. 2b). In addition, the two B_2 values of MAb-B, which are either positive or negative, coincide with each other under all pH conditions.

Our primary aim is to reveal the relationship between intermolecular interactions at low concentrations and solution properties at high concentrations of MAbs. Inter-molecular interactions at low concentration can be evaluated using AUC-SE. Our study demonstrated that B_2 values as a function of pH at concentrations lower than 10 mg/mL are in good qualitative agreement with measurements of viscosity and aggregation propensity at concentrations higher than 100 mg/mL for all three MAbs. Each MAb used in this study recognizes different antigens and has a different primary structure. Therefore, all MAbs have different pI values and amino acid compositions. This suggests that our approach could be applicable for other MAbs. Thus, for MAb solutions under physiological conditions, we can infer

that there is qualitative consistency of intermolecular interactions at low and high concentrations.

As an example of the second approach, Yadav *et al.* showed that intermolecular interactions at low concentrations of MAbs assessed by k_d derived from DLS is qualitatively inconsistent with the viscosity at high concentrations of four different MAbs (35). Based on this result, it was concluded that it is difficult to estimate physical properties at high concentrations based on behavior at low concentrations because the types of intermolecular forces change in a manner that depends on the concentrations of MAbs. This is a specific case with respect to the low ionic conditions in this previous study, but it should also be true for our MAbs if they are investigated under similar solvent conditions. At low ionic strength, electrostatic interactions among MAbs are not shielded and become significant, particularly at high concentrations. In fact, it seems that in this previous study, the intermolecular interactions observed at low concentrations that were assessed by DLS are in agreement with the intermolecular interactions observed at high concentrations that were assessed using an ultrasonic shear rheometer for all MAbs under high ionic strength conditions.

It should be noted that the k_d value obtained by DLS may be misleading with respect to the magnitude of intermolecular interactions because k_d is related not only to B_2, but also to ξ_1, which depends upon the shape and hydration state of the MAb as described in Eq. 4 (36–38). Thus, if the shape and size of the molecule change depending on the concentration, the k_d value does not reflect the only type of intermolecular interaction. On the contrary, AUC-SE directly provides a B_2 value based on the concentration dependence of $M_{W,app}$. Therefore, proper estimation of intermolecular interactions can be established. The relationship between k_d and B_2 for MAb-A, MAb-B, and MAb-C are indicated in Fig. 7. According to Eq. 4, the slope and intercept of the plot of B_2 *versus* k_d represent the $2M_W$ and hydrodynamic term $-(\xi_1+v)$, respectively. Since $2M_W$ is constant for a given MAb, the k_d value can be used for development of the formulation of the same MAb if the hydrodynamic term is significantly unchanged. However, in the case that the hydrodynamic term changes with the solution condition, k_d values under different solution conditions should be compared cautiously. For example, even in the development of the same MAb, the effect of sugar alcohols and detergents on the intermolecular interactions might meet this case. In the present study, the intercept of MAb-C is significantly different from that of the other two MAbs (Fig. 7). This result might imply that the hydrodynamic properties of MAb-C are different from those of MAb-A and MAb-B. The different hydrodynamic properties could be attributed to different hydration states and/or different three-dimensional structures.

In addition, light scattering techniques such as DLS and SLS provide an indication of both solute-solute interactions and solute-solvent interactions, whereas AUC-SE and osmometry only indicate solute-solute interactions (39,40). In fact, we observed an exception in the linear relationship between k_d and B_2. The k_d of MAb-C at pH 8 falls in a position (B_2, -1.06×10^{-5} mL·mol/g^2 and k_d, −6.9 mL/g) that deviates from the linear regression produced using values obtained at pH 5, 6, and 7. This exception might be explained by the contribution of different solvent-solute interactions.

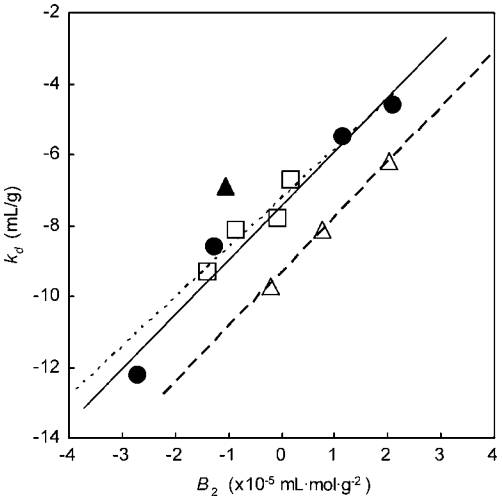

Fig. 7 Correlation of B_2 with k_d of MAb-A (●, dotted line), MAb-B (□, solid line), and MAb-C (Δ, dashed line). B_2 was obtained from AUC-SE and k_d was obtained from DLS. Regression lines were obtained from B_2 and k_d at 4 different pH values except for MAb-C, where values at pH 8 (▲) were eliminated for fitting to the regression line because of a deviation from the trend.

It is known that k_d becomes negative even if there is a repulsive interaction due to the large contribution of hydrodynamic properties (ξ_1+v) as shown in Eq. 4 (35,37). Therefore, a special conversion of k_d, which takes hydrodynamic properties into account, is required when the sign of the interaction is necessary. As shown in Fig. 8a, the viscosities of all the MAb solutions studied were found to be well correlated to the B_2 values when repulsive interactions are present (positive B_2). In the region where attractive interactions exist (negative B_2), the viscosities become larger than those in the region where repulsive interactions exist. These features are useful for the selection of MAbs and formulations of MAbs as mentioned below. Thus, AUC-SE is suitable for the assessment of intermolecular interactions.

Relationship Between Viscosity and B_2

Figure 9 describes a model of MAb self-association and aggregation via several different pathways. In pathway I, high viscosity would be induced at high concentrations due to transient cross-linked networks among MAbs formed via weak reversible self-association. The relationship between self-association of antibodies and the viscosity of antibody

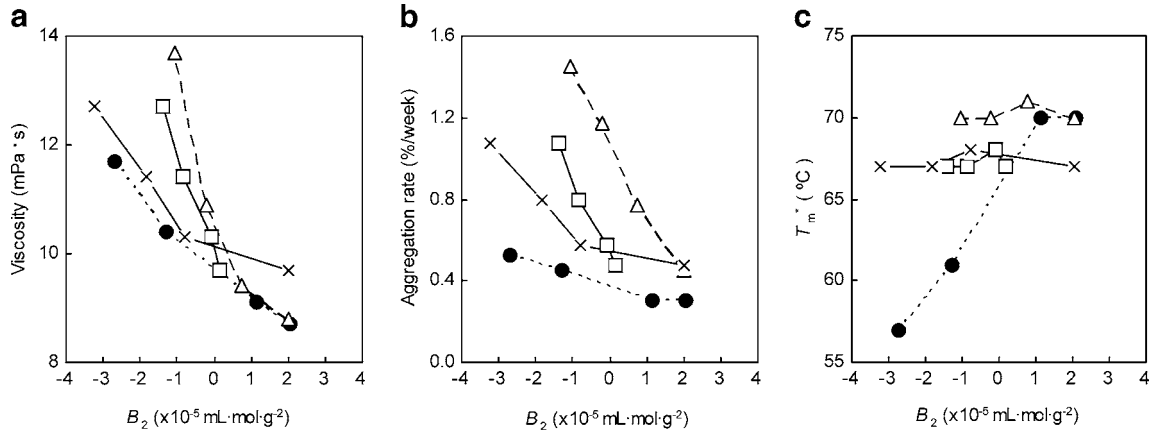

Fig. 8 Correlation of B_2 with viscosity (**a**), aggregation propensity (**b**), and thermal stability (**c**) of MAb-A (●), MAb-B (□), and MAb-C (Δ). B_2 was obtained from AUC-SE. k_d and T_m^* were obtained from DLS. Viscosities were obtained at a concentration of 150 mg/mL, and aggregates were based on SEC.

solutions has been investigated by Liu *et al.* who showed that viscosity is enhanced at about the pI and low ionic conditions in a specific IgG_1 via reversible self-association (5). Yadav *et al.* evaluated the self-association of the same IgG_1 based on the ultrasonic storage module, and suggested that short-range electrostatic interactions such as dipole-dipole and dipole-charge interactions play significant roles in highly concentrated solutions (10). A similar case was reported by Chari *et al.* for an IgG_2 (15). These intermolecular interactions attributed to the high viscosity via pathway I can be evaluated by B_2 estimated from MAb solutions in the native state at relatively low concentration, as indicated in the present study. In fact, higher viscosities

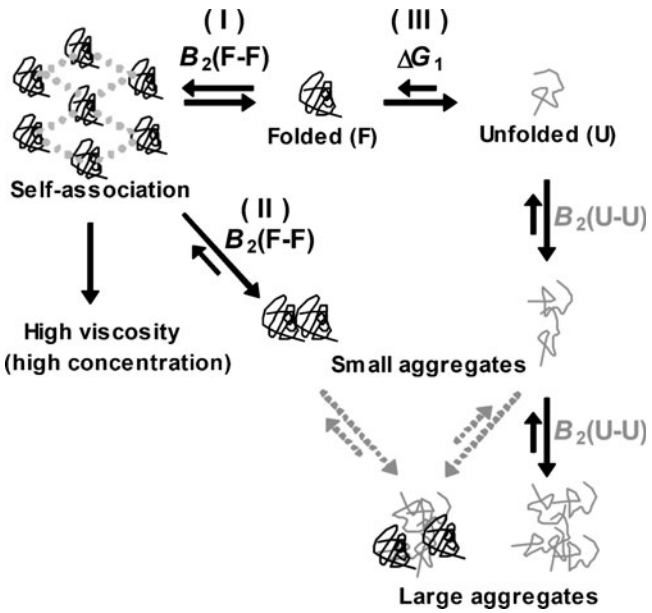

Fig. 9 Model of self-association and aggregation. B_2(F-F) is the second virial coefficient among MAbs in the folded state and B_2(U-U) is the second virial coefficient among MAbs in the unfolded state. ΔG_1 is the free energy difference between MAbs in the folded and unfolded state.

were observed at the pH levels where MAbs have lower B_2 values for all of the MAbs, as indicated in Fig. 8a (generated from the values described in Fig. 5 and Table II). These results support the presence of pathway I and indicate that B_2 (determined by AUC-SE at low concentrations) could be a reliable indicator of the viscosity of the highly concentrated MAb solution. The viscosities of three MAbs vary significantly with respect to conditions that provide larger negative B_2 values. In contrast, the viscosities of the three MAb solutions were found to have similar values as B_2 increased and finally converged under conditions that provide positive B_2 values. This behavior could be rationalized by the relationship between the intermolecular forces and the enhancement of viscosity. The major contributors of repulsive interactions of proteins are charge-charge repulsion and the excluded volume effect. In general, charge-charge repulsion is negligible in the presence of high concentrations of salt. The excluded volume is dependent on the size of the molecules and its magnitude is essentially constant for all MAbs. Thus, the viscosity of MAb is expected to be constant in the absence of any attractive interactions. On the other hand, there are various types of attractive interactions, such as dipole-dipole and hydrophobic interactions, the magnitudes of which are largely dependent on the state of the protein surface. Each MAb has a primary-order and a higher-order structure, which provide specific functions including binding to its specific antigen. Therefore, the profile of attractive intermolecular interactions is largely dependent on the constituent amino acid sequence of MAbs.

As shown in Fig. 8a, the exceptional point (B_2, 2.03×10^{-5} mL·mol/g^2 and viscosity, 9.7 mPas) was confirmed for MAb-B in the plot of B_2 *vs* viscosity when B_2 was estimated from the lower concentration range of 1 to 3 mg/mL. As mentioned above, the viscosity *vs* B_2 relationships for the three MAbs converge well when B_2 is in the concentration range of 4 to 12 mg/mL for MAb-B.

Table II Summary of Physical Parameters for MAb-A, MAb-B, and MAb-C

	pI	pH	B_2 ($\times 10^{-5}$mL mol g^{-2})	k_d (mL/g)	T_m^* (°C)	Viscosity (mPs s)	Aggregation rate (%/week)
MAb-A	6.7	5	−2.71	−12.2 ± 1.7	57	11.7	0.53
		6	−1.28	−8.6 ± 0.9	61	10.4	0.45
		7	1.15	−5.5 ± 1.1	70	9.1	0.30
		8	2.08	−4.6 ± 0.3	70	8.7	0.30
MAb-B	8.9	5	0.34 (2.03)	−6.7 ± 0.5	67	9.7	0.48
		6	−0.72 (−0.77)	−7.8 ± 0.2	68	10.3	0.58
		7	−1.15 (−1.83)	−8.1 ± 1.0	67	11.4	0.80
		8	−1.49 (−3.21)	−9.3 ± 1.0	67	12.7	1.08
MAb-C	8.8	5	2.03	−6.2 ± 1.0	70	8.8	0.45
		6	0.76	−8.1 ± 1.2	71	9.4	0.78
		7	−0.22	−9.7 ± 0.9	70	10.9	1.18
		8	−1.06	−6.9 ± 0.2	70	13.7	1.45

B_2 was obtained from AUC-SE. For MAb-B, B2 was obtained from the concentrations of 1, 2, and 3 mg/mL (in parenthesis), and 5, 7.5, and 10 mg/mL. k_d and T_m^* were obtained from DLS. Viscosities were obtained at a concentration of 150 mg/mL, and aggregation rate was estimated from SEC

These results suggest that B_2 values estimated from rather high concentrations might be suitable for predicting the viscosity at high concentrations, although the higher virial coefficient would be necessary in the case of highly concentrated solutions.

Relationship Between Aggregation Propensity and B_2

To predict the aggregation propensity of antibody solutions, the physical properties of the antibodies must be assessed in terms of colloidal stability and conformational stability. Colloidal stability is attributed to intermolecular interactions where improved stability arises from repulsive intermolecular interactions. On the other hand, conformational stability is attributed to a free energy difference, ΔG, between folded (F) and unfolded (U) states of protein where improved stability arises from a larger ΔG. Each aspect of stability is related to aggregation via different pathways, as shown in Fig. 9 (17,41,42). One major pathway (pathway II), which is related to colloidal stability, is initiated by reversible self-association of a MAb in the folded state. The other pathway (pathway III), which is related to conformational stability, is initiated by structural and chemical changes resulting in the accumulation of MAb in the unfolded state, followed by successive formation of large aggregates via the formation of small aggregates. In the present study, aggregation was observed to accelerate under conditions that provide a large negative B_2 corresponding to the presence of more attractive intermolecular interactions in all MAbs (Fig. 8b). However, the relationship between B_2 and aggregation propensity is limited and rather qualitative. These results suggest that colloidal stability is related to the formation of aggregates as previously mentioned (17,41) and B_2, estimated from AUC-SE of MAbs solutions at low concentrations, is an effective indicator of stability for highly concentrated solutions. The aggregation propensity showed a similar trend with respect to viscosity by indicating that different MAbs have similar aggregation propensity values as B_2 increases. This behavior might be accounted for by the same mechanism that is functioning in the case of viscosity.

Conformational stability provided by pathway III, in which the difference in free energy between folded and unfolded states contributes to aggregation, was investigated based on the thermal stability assessed by DLS (Fig. 5 and Table II). In this pathway, intermolecular interactions among MAbs in the folded state (represented as B_2(F-F)) do not contribute to the formation of aggregates, whereas intermolecular interactions between unfolded states (represented as B_2(U-U)) contribute to the formation of aggregates (Fig. 9). B_2 values determined by AUC-SE at ambient temperature do not reflect aggregation occurring via pathway III. In fact, there is no significant correlation observed between B_2 and T_m^* (Fig. 8c). In one exception, B_2 showed good qualitative agreement with T_m^* in MAb-A. In this case, intermolecular interactions between MAbs in the unfolded state could be attributed to B_2 because the population in the unfolded state should be larger in MAbs with smaller T_m^* values.

In conclusion, B_2 determined by AUC-SE is a qualitative indicator for aggregation via the pathway initiated by the self-association of MAbs. This pathway is considered to contribute to the formation of aggregates during storage. This is not a stressing condition where unfolding is slightly induced. Therefore, it is useful to select formulations of MAbs that have promising stability. On the other hand, aggregation via the pathway initiated by unfolding did not necessarily correlate with B_2. In this case, a combination of B_2 and T_m

determined by DLS and/or other techniques, such as differential scanning calorimetry, will provide effective information for estimating the aggregation propensity.

Selection of Antibodies and Formulations Based on B_2

Selection of optimal formulations and MAbs with superior physical properties are important for the development of therapeutic MAbs. AUC-SE provides useful information in terms of viscosity and aggregation propensity. As mentioned in the Results section, the pH dependence of B_2 (as measured by AUC-SE) is in good qualitative agreement with the dependence of B_2 on viscosity and aggregation propensity in all MAbs. Here, we propose an approach to select a formulation with more positive or less negative B_2 values. Additionally, for the selection of MAbs with superior physicochemical properties from various candidate MAbs, B_2 can serve as an effective indicator. Positive B_2 values were found to be quantitatively consistent with viscosity regardless of the type of MAbs (Fig. 8a). Therefore, selection of MAbs with more positive B_2 values will be a good approach to achieve lower viscosity in highly concentrated MAb solutions. On the other hand, negative B_2 values were quantitatively inconsistent with viscosity when different MAbs were compared. In addition, there was no quantitative correlation between B_2 and aggregation propensity among different MAbs regardless of the negative or positive B_2 values. In this case, B_2 values of different formulations should be examined in order to assess the possibility of improving formulations by optimization. Herein, we suggest assessing the pH dependence of B_2 and selecting MAbs that have more positive or less negative B_2 values in acidic pH. MAb-B and MAb-C are examples of such MAbs. Major degradation, including deamidation of proteins, is accelerated under basic conditions; therefore, formulations with high pH levels are not preferable. Thus, MAbs that are more stable under acidic conditions are suitable as therapeutic MAbs. Conclusively, B_2 determined by AUC-SE provides an opportunity to identify appropriate formulations and MAbs with favorable physical properties from small amounts of samples at low concentrations, thereby reducing the time required for developing therapeutic MAbs.

CONCLUSION

Aggregation and viscosity are difficult problems to overcome in the development of therapeutic antibodies. Therefore, a reliable strategy for the prediction of viscosity and aggregation propensity in the evaluation of antibody solutions is an important requirement. In this study, we investigated the intermolecular interaction of MAbs by determining B_2 from AUC-SE measurements. As a whole, we ensured that the intermolecular interactions at low concentrations are qualitatively comparable to those determined at high concentrations. In fact, B_2 determined by AUC-SE was in good qualitative accordance with viscosity and aggregation propensity for all the MAb solutions studied. In particular, the correlation was confirmed by the finding that repulsive interactions dominate when B_2 values are positive. However, the relationship was found to be only qualitative in the presence of attractive interactions that are indicated by negative B_2 values. We also determined (based on the comparison of AUC-SE data with DLS data) that AUC-SE provides B_2 values that are qualitatively consistent with viscosity and aggregation propensity. A good qualitative relationship was confirmed between B_2 determined from AUC-SE and k_d determined from DLS. AUC-SE and DLS have been widely used for the evaluation of dispersion in protein solutions. However, an exception was observed in the correlation of k_d with viscosity and aggregation propensity. These results indicate that B_2 determined from AUC-SE is a better indicator for the estimation of the viscosity and aggregation propensity of highly concentrated solutions. Although AUC-SE is recognized as a low throughput technique, the information obtained from this technique is highly valuable and can provide useful details about the type of dominant intermolecular interactions and the critical physical parameters of a target therapeutic protein.

ACKNOWLEDGMENTS & DISCLOSURES

The authors would like to thank Daisuke Ama, Kei Kubota, Yuki Araki, Mami Mitsui and Misako Sawakuri (Daiichi Sankyo Co., Ltd., Tokyo, Japan) for their skillful technical support.

REFERENCES

1. Reichert JM, Rosensweig CJ, Faden LB, Dewitz MC. Monoclonal antibody successes in the clinic. Nat Biotechnol. 2005;23(9):1073–8.
2. Shire SJ, Shahrokh Z, Liu J. Challenges in the development of high protein concentration formulations. J Pharm Sci. 2004;93(6):1390–402.
3. Treuheit MJ, Kosky AA, Brems DN. Inverse relationship of protein concentration and aggregation. Pharm Res. 2002;19(4):511–6.
4. Jiménez M, Rivas G, Minton AP. Quantitative characterization of weak self-association in concentrated solutions of immunoglobulin G via the measurement of sedimentation equilibrium and osmotic pressure. Biochemistry. 2007;46:8373–8.
5. Liu J, Nguyen MDH, Andya JD, Shire SJ. Reversible self-association increases the viscosity of a concentrated monoclonal antibody in aqueous solution. J Pharm Sci. 2005;94(9):1928–40.

6. Minton AP. The influence of macromolecular crowding and macromolecular confinement on biochemical reactions in physiological media. J Biol Chem. 2001;276(14):10577–80.
7. Minton AP. Influence of macromolecular crowding upon the stability and state of association of proteins: predictions and observations. J Pharm Sci. 2005;94(8):1668–75.
8. Harn N, Allan C, Oliver C, Middaugh CR. Highly concentrated monoclonal antibody solutions: direct analysis of physical structure and thermal stability. J Pharm Sci. 2007;96(3):532–46.
9. Kamerzell TJ, Kanai S, Liu J, Shire SJ, Wang YJ. Increasing IgG concentration modulates the conformational heterogeneity and bonding network that influence solution properties. J Phys Chem. 2009;113:6109–18.
10. Yadav S, Liu J, Shire SJ, Kalonia DS. Specific interactions in high concentration antibody solutions resulting in high viscosity. J Pharm Sci. 2010;99(3):1152–68.
11. Kanai S, Liu J, Patapoff TW, Shire SJ. Reversible self-association of a concentrated monoclonal antibody solution mediated by Fab–Fab interaction that impacts solution viscosity. J Pharm Sci. 2008;97(10):4219–27.
12. Zhang J, Liu XY. Effect of protein-protein interactions on protein aggregation kinetics. J Chem Phys. 2003;119(20):10972–6.
13. Saluja A, Badkar AV, Zeng DL, Kalonia DS. Ultrasonic rheology of a monoclonal antibody (IgG_2) solution: implications for physical stability of proteins in high concentration formulations. J Pharm Sci. 2007;96(12):3181–95.
14. Alford JR, Kwok SC, Roberts JN, Wuttke DS, Kendrick BS, Carpenter JF, *et al.* High concentration formulations of recombinant human Interleukin-1 receptor antagonist: I. Physical characterization. J Pharm Sci. 2008;97(8):3035–50.
15. Chari R, Jerath K, Badkar AV, Kalonia DS. Long- and short-range electrostatic interactions affect the rheology of highly concentrated antibody solutions. Pharm Res. 2009;26(12):2607–18.
16. Mahler HC, Friess W, Grauschopf U, Kiese S. Protein aggregation: pathways, induction factors and analysis. J Pharm Sci. 2009;98(9):2909–34.
17. Chi EY, Krishnan S, Randolph TW, Carpenter JF. Physical stability of proteins in aqueous solution: mechanism and driving forces in nonnative protein aggregation. Pharm Res. 2003;20 (9):1325–36.
18. Gokarn YR, Fesinmeyer RM, Saluja A, Cao S, Dankberg J, Goetze A, *et al.* Ion-specific modulation of protein interactions: anion-induced, reversible oligomerization of a fusion protein. Protein Sci. 2009;18(1):169–79.
19. Nishi H, Miyajima M, Nakagami H, Noda M, Uchiyama S, Fukui K. Phase separation of an IgG1 antibody solution under a low ionic strength condition. Pharm Res. 2010;27(7):1348–60.
20. Salinas BA, Sathish HA, Bishop SM, Harn N, Carpenter JF, Randolph TW. Understanding and modulating opalescence and viscosity in a monoclonal antibody formulation. J Pharm Sci. 2010;99(1):82–93.
21. Wu SJ, Luo J, O'Neil KT, Kang J, Lacy ER, Canziani G, *et al.* Structure-based engineering of a monoclonal antibody for improved solubility. Protein Eng Des Sel. 2010;23(8):643–51.
22. Nezlin R. Interactions between immunoglobulin G molecules. Immunol Lett. 2010;132(1–2):1–5.
23. Saluja A, Badkar AV, Zeng DL, Nema S, Kalonia DS. Ultrasonic storage modules as a novel parameter for analyzing protein-protein interactions in high protein concentration solutions: correlation with static and dynamic light scattering measurements. Biophys J. 2007;92:234–44.
24. Holde KE, Johnson C, Ho PS. Principles of physical biochemistry. Upper Saddle River: Pearson Education; 2006.
25. Neal BL, Asthagiri D, Lenhoff AM. Molecular origins of osmotic second virial coefficients of proteins. Biophys J. 1998;75:2469–77.
26. Attri AK, Minton AP. New methods for measuring macromolecular interactions in solution via static light scattering: basic methodology and application to nonassociating and self-associating proteins. Anal Biochem. 2005;337:103–10.
27. Alford JR, Kendrick BS, Carpenter JF, Randolph TW. Measurement of the second osmotic virial coefficient for protein solutions exhibiting monomer-dimer equilibrium. Anal Biochem. 2008;377:128–33.
28. Narayanan J, Liu XY. Protein interactions in undersaturated and supersaturated solutions: a study using light and X-ray scattering. Biophys J. 2003;84:523–32.
29. Brun VL, Friess W, Bassarab S, Mühlau S, Garidel P. A critical evaluation of self-interaction chromatography as a predictive tool for the assessment of protein-protein interactions in protein formulation development: a case study of a therapeutic monoclonal antibody. Eur J Pharm Biopharm. 2010;75(1):16–25.
30. Brun VL, Friess W, Bassarab S, Garidel P. Correlation of protein-protein interactions as assessed by affinity chromatography with colloidal protein stability: a case study with lysozyme. Pharm Dev Technol. 2010;15(4):421–30.
31. Harding SE, Rowe AJ, Horton JC. Analytical ultracentrifugation in biochemistry and polymer science. London: Royal Society of Chemistry; 1992. p. 90–125.
32. McGown EL, Hafeman DG. Multichannel pipettor performance verified by measuring pathlength of reagent dispensed into a microplate. Anal Biochem. 1998;258:155–7.
33. Sahin E, Grillo AO, Perkins MD, Roberts CJ. Comparative effects of pH and inonic strength on protein-protein intaractions, unfolding, and aggregation for IgG1 antibodies. J Pharm Sci. 2010;99(12):4830–48.
34. Engelsman J, Garidel P, Smulders R, Koll H, Smith B, Bassarab S, *et al.* Strategies for the assessment of protein aggregates in pharmaceutical biotech product development. Pharm Res. 2011;28(4):920–33.
35. Yadav S, Shire SJ, Kalonia DS. Factors affecting the viscosity in high concentration solutions of different monoclonal antibodies. J Pharm Sci. 2010;99(12):4812–29.
36. Frost RA, Caroline D. Diffusion of polystyrene in a theta mixed solvent (Benzene-2-Propanol) by Photon-correlation spectroscopy. Macromolecules. 1976;10(3):616–8.
37. Yamakawa H. Concentration dependence of the frictional coefficient of polymers in solution. 1962;36(11):2995–3001.
38. Lehermayr C, Mahler HC, Mäder K, Fischer S. Assessment of net charge and protein–protein interactions of different monoclonal antibodies. J Pharm Sci. 2011;100(7):2551–62.
39. Winzor DJ, Deszczynski M, Harding SE, Wills PR. Nonequivalence of second virial coefficients from sedimentation equilibrium and static light scattering studies of protein solutions. Biophys Chem. 2007;128:46–55.
40. Deszczynski M, Harding SE, Winzor DJ. Negative second virial coefficients as predictors of protein crystal growth: evidence from sedimentation equilibrium studies that refutes the designation of those light scattering parameters as osmotic virial coefficients. Biophys Chem. 2006;120:106–13.
41. Chi EY, Krishnan S, Kendrick BS, Chang BS, Carpenter JF, Randolph TW. Roles of conformational stability and colloidal stability in the aggregation of recombinant human granulocyte colony-stimulating factor. Protein Sci. 2003;12:903–13.
42. Hawe A, Kasper JC, Friess W, Jiskoot W. Structural properties of monoclonal antibody aggregates induced by freeze-thawing and thermal stress. Eur J Pharm Sci. 2009;38:79–87.